Statistical representation of intrinsic electronic tunneling characteristics through alkyl self-assembled monolayers in nanowell device structures

Hyunwook Song and Takhee Lee[a)]
Department of Materials Science and Engineering, Gwangju Institute of Science and Technology, Gwangju 500-712, Korea

Nak-Jin Choi and Hyoyoung Lee
National Creative Research Initiative, Center for Smart Molecular Memory, Electronics and Telecommunications Research Institute, Daejeon 305-350, Korea

Systematic electronic transport measurements in nanometer-scale junctions containing self-assembled monolayers of alkyl molecules are reported using nanowell device structures. The comprehensive temperature-variable current-voltage characterizations and statistical analysis for the acquired transport data show that direct tunneling indeed can be assigned as the dominant charge transport mechanism of the alkyl monolayers in a voltage range $\leqslant \pm 1$ V. The intrinsic tunneling characteristics of alkyl molecular junctions are examined by excluding other parasitic conduction mechanisms by the data analyses and statistically defining representative data. The demonstrated intrinsic tunneling characteristics are well consistent with numerous previous reports for alkyl-based monolayers. The current characteristics are temperature independent and exponentially depend on the molecular length. The tunneling decay coefficient is determined as $0.83–0.73$ Å^{-1} in the bias range from 0.1 to 1.0 V and is independent of temperature. The statistical histogram of current densities for all direct tunneling devices exhibits log-normal distribution, which is likely due to a variation in tunneling distance. © *2008 American Vacuum Society.* [DOI: 10.1116/1.2905237]

I. INTRODUCTION

Self-assembled organic molecules are promising candidates as future high-density and low-cost electronic device components because of their extremely small size, chemical tunability, and spontaneous formation of robust molecular monolayers.[1,2] However, despite there being abundant potential virtues as compared with conventional silicon-based microelectronics, molecular electronic device applications have been hindered by the difficulty to achieve reliable, consistent, and reproducible electronic transport characterization of molecular systems. For instance, large discrepancies have been observed in both the experimental data and theoretical modeling on even nominally identical molecules and testbeds.[3,4] For the ultimate realization of molecular-scale electronic devices, the intrinsic nature of electronic transport through the organic molecules bridged between metallic (or semiconductor) contacts is of primary importance[5–8] in which their charge transport properties are determined by molecules incorporated in the junctions, but not by other parasitic effects such as unintentional defects or leakage paths. Specifically, alkyl-based molecular junctions are beneficial to examine the intrinsic transport properties because many reports have extensively characterized this molecular system.

Here, we report on the systematic electronic transport measurements in nanometer-scale junctions containing self-assembled monolayers (SAMs) of alkyl molecules, which are well-studied molecular systems consisting of saturated C–C bonds of sp^3 hybridization terminated by linkers (e.g., thiol groups) that can bind to electrodes. These molecules have very short molecular lengths $(1–2$ nm) and large gaps $(\sim 8$ eV) between their highest occupied molecular orbital (HOMO) and lowest unoccupied molecular orbital (LUMO). For alkyl-based junctions, thereby, the conduction mechanism can be described as a simple classical tunneling via metal-insulator-metal (MIM) junctions and this has been consistently confirmed by many former reports.[9–13] These well-understood molecular assemblies can serve as a standard model for eliminating (or appreciating) uncontrolled stochastic variables on molecular transport characterization. In this study, further emphasis is made on examining the intrinsic tunneling characteristics through the alkyl monolayers. The authors' previous experiments with alkanethiol SAMs have shown how to determine the intrinsic transport properties of molecular devices.[11] The comprehensive temperature-variable current-voltage $[I(V,T)]$ characterization for candidate molecular devices monitors the full spectrum of transport properties and subsequent statistical analysis determines the most probable measured characteristics as an intrinsic molecular signature. The $I(V,T)$ characterization is necessary to unambiguously assign the conduction mechanism, for example, to distinguish electronic tunneling transport from other transports such as impurity-mediated transport or thermionic emission.[9,10] Furthermore, studies based on the statistical approach[13–17] would provide objective criteria in characterizing the intrinsic transport properties, thus
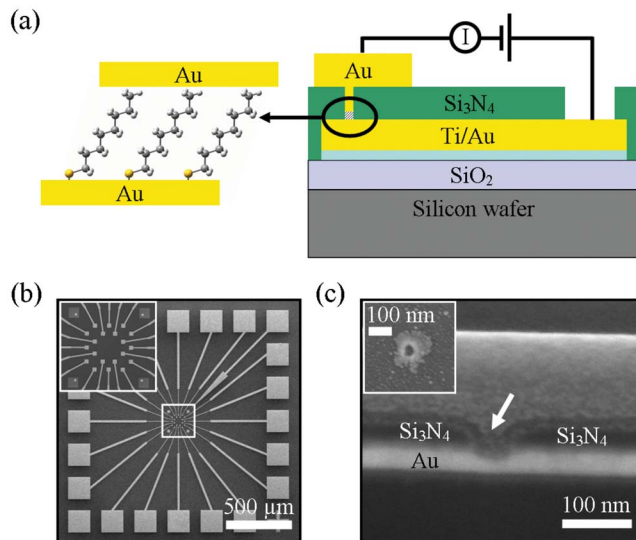
[a)]Electronic mail: tlee@gist.ac.kr

FIG. 1. (a) Schematic of the molecular device structure. (b) SEM image of a fabricated die containing 20 molecular devices in top view. The inset shows an array of 20 bottom electrodes, corresponding to a white box area. (C) SEM image of a nanowell (marked by the arrow) in cross-sectional view before the deposition of the SAMs and top metal electrode. The inset shows a nanowell in top view.

FIG. 2. Schematics of the possible *I(V)* curves of the molecular devices. (a) a short junction, (b) an open junction, and (c) a metal-molecule-metal junction.

reducing the discrepancies in molecular transport characterizations and providing more accurate transport parameters through molecular monolayers.

II. EXPERIMENT

We used mass-fabricated molecular devices with an array of nanowell structures,[18] which are a planar device and do not need a back side processing as opposed to the through-wafer devices.[9,10] Thus, the fabrication is readily compatible with current complementary metal-oxide semiconductor technology and large-scale integration. In this device structure, as schematically illustrated in Fig. 1(a), alkanethiol SAMs are sandwiched between two metallic contacts, creating a vertical type of metal-molecule-metal junctions. Note that all devices were fabricated on a single silicon wafer at the same time in a single fabrication process run. This can minimize unintentional deviation which may stem from the different fabrication runs on separate substrates. The device fabrication started with the formation of bottom electrodes (5 nm Ti/50 nm Au) on a 4 in. silicon wafer with a 500-nm-thick layer of SiO_2 by standard photolithography and lift-off process. A 50-nm-thick Si_3N_4 film was then deposited on the silicon wafer that had the prepatterned bottom electrodes for device isolation using plasma-enhanced chemical vapor deposition. The bottom electrodes are arrayed in the center of the device structure connected with probe contact pads in the outer sides, as shown in the scanning electron microscopy (SEM) image of Fig. 1(b). Subsequent electron-beam lithography and reactive ion etching were used to form nanowell structures through the Si_3N_4 layer. The Au surface of the bottom electrode was exposed through the nanowell. Figure 1(c) shows a cross-sectional SEM image of a nanowell from which the diameter of the
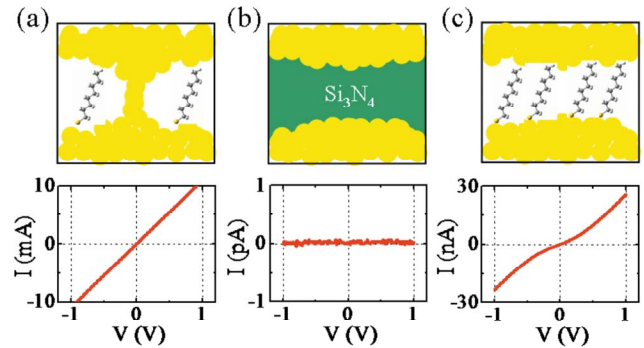
nanowell was estimated to be ~50 nm. After cleaning with piranha solution (30% hydrogen peroxide added to 66% sulfuric acid in a ratio of 1:3), the wafer was then transferred into a molecular solution to deposit the molecular monolayer on the exposed Au surface of the bottom electrode through the nanowell. For molecular deposition, a 5 mM solution of alkanethiol was prepared in 10 ml ethanol. The deposition was done on Au surface in solution for 1−2 days inside a nitrogen-filled glovebox with an oxygen level less than 10 ppm to avoid unintentional incorporations of impurities in the devices. Alkanethiols (from Sigma-Aldrich) of various molecular lengths, octanethiol $[CH_3(CH_2)_7SH$, denoted as C8, for the number of alkyl units], dodecanethiol $[CH_3(CH_2)_{11}SH, C12]$, and hexadecanethiol $[CH_3(CH_2)_{15}SH, C16]$ were used to form the active molecular components. Before use, each sample was rinsed with a few milliliters of ethanol and gently blown dry in a stream of nitrogen to remove noncovalently attached alkanethiol molecules on Au surface. As an example, the chemical structure of octanethiol is shown in Fig. 1(a). As the last step, top electrode (50-nm-thick Au) was deposited using a shadow mask. All electrical measurements were performed in a voltage range ⩽±1 V using a semiconductor characterization system (Keithley 4200) in a temperature-variable cryogenic probe station (Measure Jig Co., model WM-365B).

III. RESULTS AND DISCUSSION

A. Electronic transport mechanism of alkanethiols

We examined molecular devices fabricated as the nanowell structure shown in Fig. 1, employing alkanethiol SAMs of various molecular chain lengths. As a screening process for nonworking devices,[14] room temperature *I(V)* measurements were executed before cooling in the cryogenic probe station. Figure 2 shows schematics of molecular devices with corresponding experimental *I(V)* curves obtained at room temperature. In an electrically shorted junction [Fig. 2(a)], linear *I(V)* curves are shown with current in the milliampere range, which is caused by the penetration of the vapor-deposited top electrode through the molecular monolayer, making a direct contact with the bottom electrode. In contrast, Fig. 2(b) indicates an open junction with no detectable current in the
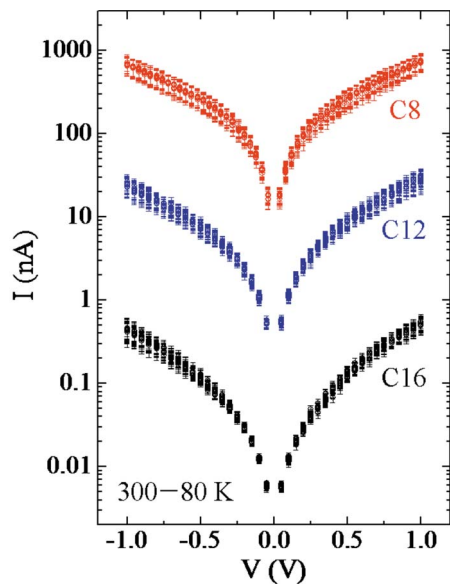
FIG. 3. The average of $I(V,T)$ characteristics for each alkanethiol SAM (C8, C12, and C16) as the representative data of 108 direct tunneling devices. 31 devices for C8, 42 devices for C12, and 35 devices for C16, respectively. The $I(V,T)$ data at temperature from 300 to 80 K with 20 K step are plotted on a semilogarithmic scale.

FIG. 4. (a) Arrhenius plot generated from the $I(V,T)$ data in Fig. 3, at voltages from 0.1 to 1.0 V with 0.1 V step. (b) Plot of $\ln(I/V^2)$ vs $1/V$ at temperature from 300 to 80 K with 20 K step.

subpicoampere range, which is likely due to a failure during the device fabrication such as an incomplete etching of the Si_3N_4 insulating layer. The characteristic signature of metal-molecule-metal junctions under investigation is shown in Fig. 2(c). The current flow is in the nanoampere range and the $I(V)$ characteristics exhibit a nonlinear behavior. To determine the conduction mechanism from the candidate molecular devices exhibiting the characteristic behaviors typically in Fig. 2(c), we performed the comprehensive $I(V,T)$ characterizations and subsequent statistical analysis for the acquired transport data. For reliability, we only considered the devices where the conduction mechanism is confirmed by the repeated $I(V)$ measurements in a sufficient wide temperature range (300–80 K). As a result, among a total of 123 molecular devices that were measured with $I(V,T)$ characterization, most devices (108 devices; 87.8%) showed indeed the direct tunneling characteristics (from $V=-1$ to 1 V).[19] The dominance of direct tunneling in alkanethiol SAMs is in good agreement with previous results[9,10] and can be reasonably anticipated due to large HOMO-LUMO gap (~8 eV) with a short molecular length.

B. Statistical representation of intrinsic tunneling characteristics through alkanethiols

Figure 3 shows the average of $I(V,T)$ characteristics for each of different length alkanethiol SAMs as the representative data of 108 direct tunneling devices. The error bars on each data give the standard deviation upon the averaging. The devices exhibiting other parasitic conduction mechanisms are thoroughly excluded on the analyses so that the representative data would demonstrate the intrinsic molecular electronic properties responsible for dominating tunneling
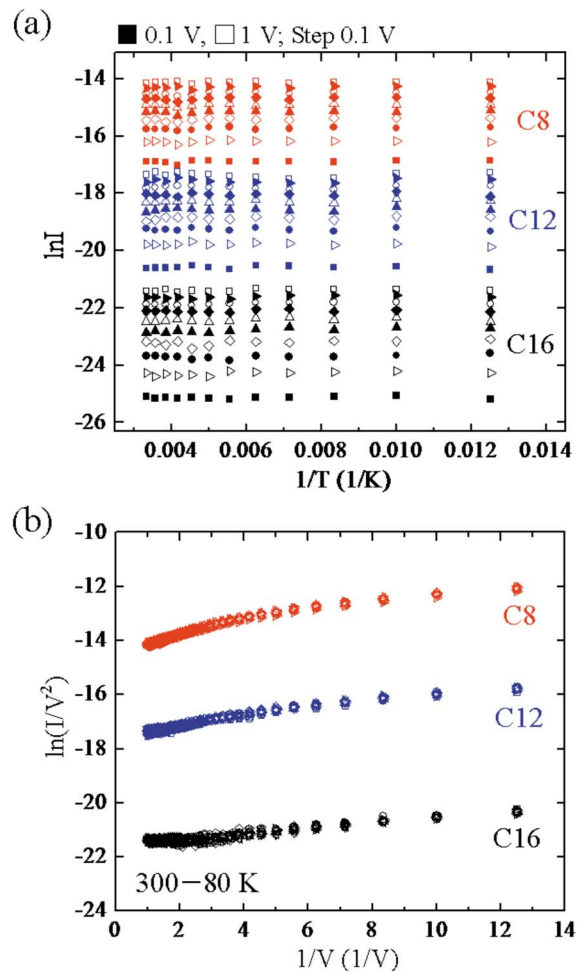
conduction mechanism. In Fig. 3, no significant temperature dependence of the characteristics is observed over the range from 300 to 80 K. An Arrhenius plot $[\ln(I)$ vs $1/T]$ of this is shown in Fig. 4(a), exhibiting little temperature dependence in the slopes of $\ln(I)$ vs $1/T$ at different biases and thus indicating the absence of thermal activation. Based on the applied bias as compared to barrier height (Φ_B), the tunneling transports can be divided into direct tunneling ($V < \Phi_B/e$) or Fowler-Nordheim tunneling ($V > \Phi_B/e$) regimes.[9] These two tunneling mechanisms can be distinguished by their distinct current-voltage dependencies.[20] The molecular devices in direct tunneling do not exhibit an inflection point on a plot of $\ln(I/V^2)$ vs $1/V$ as shown in Fig. 4(b). This is consistent with tunneling through a trapezoidal barrier when the applied bias is less than the barrier height.[21]

Length-dependent tunneling behavior was also examined using the direct tunneling devices of different length alkanethiols.[9–14,16] The current density J through alkanethiol SAMs has shown an exponential dependence on the barrier width d as[16,22,23]
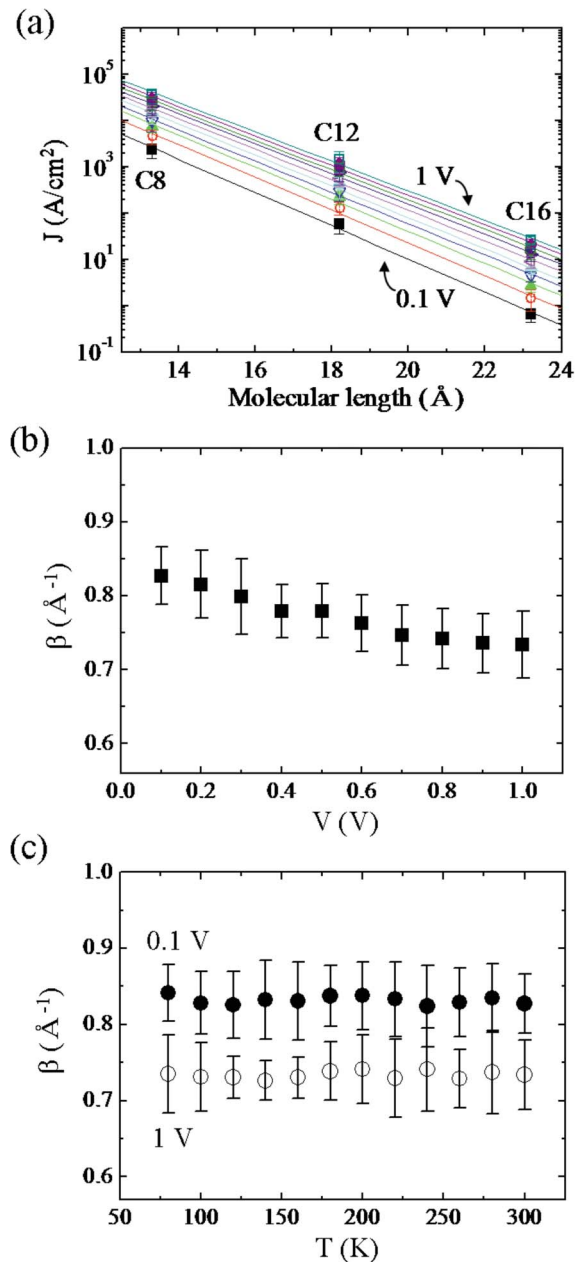
(a)

(b)

(c)

FIG. 5. (a) Semilogarithmic plot of tunneling current densities at 300 K (from Fig. 3) vs molecular lengths. The lines through the data points are linear fittings. (b) Bias dependence of β values. (c) Plot of β values at 0.1 and 1.0 V as a function of temperature.

$$J \propto \exp(-\beta d), \qquad (1)$$

where β is tunneling decay coefficient dependent on molecular structure,[23] and d is molecular length which is the width for the tunneling barrier, by assuming the through-bond tunneling, i.e., the current flows along the tilted molecular chain between the metal contacts.[24] Molecular lengths used in the analysis are 13.3, 18.2, and 23.2 Å for the C8, C12, and C16 alkanethiols, respectively. Each molecular length was determined by adding a Au-thiol bonding length to the length of molecule.[23] The current densities were calculated by using the junction area of ~50 nm in diameter. In Fig. 5(a), the
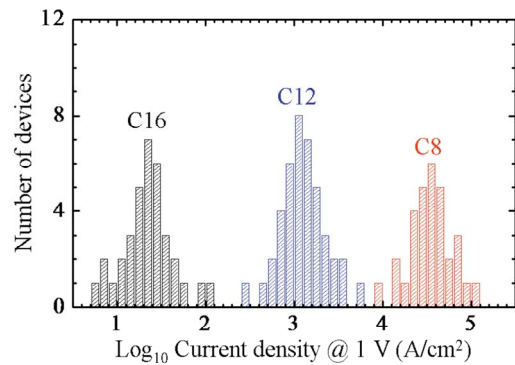

FIG. 6. Histogram plot for observed current densities of all the direct tunneling C8, C12, and C16 molecular devices (108 devices).

current densities at 300 K are plotted on a semilogarithmic scale as a function of the molecular length at various voltages. The error bars represent the standard deviation upon averaging over the calculated current densities of 108 direct tunneling devices. According to Eq. (1), the decay coefficient β can be determined from the slope of the linear fits in Fig. 5(a). The results are displayed in Fig. 5(b). This gives a β value from 0.83 to 0.73 Å^{-1} in the bias range from 0.1 to 1.0 V. These β values are in good agreement with those reported previously.[9–14,16,22] The uncertainty of an individual β value in this plot was obtained by considering the linear fitting errors. The decrease of β with increasing bias was also observed, which results from the barrier lowering effect due to applied bias.[9,10,12] Figure 5(c) shows a plot of β values at 0.1 and 1.0 V as a function of temperature, indicating no specific temperature dependence of β values.

C. Statistical distribution of current density

Repeated measurements offer a statistical picture of molecular transport properties, typically presented as histograms. Figure 6 shows the statistical histogram of the current densities for the direct tunneling devices of different length alkanethiols (marked as C16, C12, and C8, respectively) calculated at 1 V. Depending on the molecular length of alkanethiols, the current density values vary over orders of magnitude and appear to be distributed log normally, i.e., the logarithms of the current densities are distributed as a normal bell curve.[25] The statistical distribution that we observed (Fig. 6) indicates that there are fluctuation factors causing such statistical distribution of tunneling currents in molecular junctions. Particularly, one can note that the histograms in Fig. 6 show the distribution of the logarithmic current densities, indicating the existence of a fluctuation factor causing the exponential distribution in the current densities. This fluctuation factor could be the tunneling distance, indicating that fluctuations in molecular configurations in the self-assembled monolayers in the device junctions are possible, such as molecular tilting angle, molecular orientations, alkyl-Au binding sites, and surface flatness of the Au bottom electrode on which the molecules are assembled.[14,15,25–27] The dimensional variation such as variation in junction area

may exist, but the area fluctuation does not produce an exponential distribution in current; instead, fluctuation in the tunneling path is probably responsible for the distribution data of Fig. 6. The log-normal distribution of current densities was not observed in the absence of molecules. Instead, the current densities of the devices without molecules showed a linear normal distribution in the histogram (not shown here), mostly resulting from a variation of the junction area.

IV. CONCLUSION

We examined the intrinsic electronic tunneling characteristics through alkanethiol SAMs using nanowell devices. The intrinsic molecular transport properties can be determined by exhaustively excluding other observed parasitic conduction mechanisms with $I(V,T)$ characterization. Among the 123 measured alkanethiol molecular devices, most devices (108 devices, 87.8%) showed the direct tunneling transport as the dominant charge conduction mechanism. From the subsequent statistical analysis, the representative data of alkanethiols can be determined by averaging 108 direct tunneling devices. The statistical histogram of current densities based on 108 direct tunneling devices showed log-normal distribution in current density values, which is the result of a variation in tunneling distance.

ACKNOWLEDGMENTS

[1]*Molecular Nanoelectronics*, edited by M. A. Reed and T. Lee (American Scientific, Stevenson Ranch, CA, 2003).

[2]*Introducing Molecular Electronics*, edited by G. Cuniberti, G. Fagas, and K. Richter (Springer, Berlin, 2005).

[3]A. Salomon, D. Cahen, S. Lindsay, J. Tomfohr, V. B. Engelkes, and C. D. Frisbie, Adv. Mater. (Weinheim, Ger.) **15**, 1881 (2003).

[4]S. M. Lindsay and M. A. Ratner, Adv. Mater. (Weinheim, Ger.) **19**, 23 (2007).

[5]A. Nitzan and M. A. Ratner, Science **300**, 1384 (2003).

[6]N. J. Tao, Nat. Nanotechnol. **1**, 173 (2006).

[7]S. Lodha and D. B. Janes, J. Appl. Phys. **100**, 024503 (2006).

[8]A. Scott, C. Risko, M. A. Ratner, and D. B. Janes, Appl. Phys. Lett. **91**, 033508 (2007).

[9]W. Wang, T. Lee, and M. A. Reed, Phys. Rev. B **68**, 035416 (2003).

[10]W. Wang, T. Lee, and M. A. Reed, Rep. Prog. Phys. **68**, 523 (2005).

[11]H. Song, T. Lee, N.-J. Choi, and H. Lee, Appl. Phys. Lett. **91**, 253116 (2007).

[12]H. B. Akkerman, P. W. M. Blom, D. M. de Leeuw, and B. de Boer, Nature (London) **441**, 69 (2006).

[13]X. Li, J. He, J. Hihath, B. Xu, S. M. Lindsay, and N. J. Tao, J. Am. Chem. Soc. **128**, 2135 (2006).

[14]T. W. Kim, G. Wang, H. Lee, and T. Lee, Nanotechnology **18**, 315204 (2007).

[15]E. Lörtscher, H. B. Weber, and H. Riel, Phys. Rev. Lett. **98**, 176807 (2007).

[16]S.-Y. Jang, P. Reddy, A. Majumdar, and R. A. Segalman, Nano Lett. **6**, 2362 (2006).

[17]M. T. González, S. Wu, R. Huber, S. J. Molen, C. Schönenberger, and M. Calame, Nano Lett. **6**, 2238 (2006).

[18]N. Majumdar *et al.*, J. Vac. Sci. Technol. B **23**, 1417 (2005).

[19]Among the 123 $I(V,T)$ transport data acquired, we observed four different transport mechanisms, i.e., direct tunneling (108 devices, 87.8%), Fowler–Nordheim tunneling (8 devices, 6.5%), thermally activated conduction (5 devices, 4.1%), and Coulomb blockade phenomenon (2 devices, 1.6%). Also see Ref. 11.

[20]S. M. Sze, *Physics of Semiconductor Devices*, 2nd ed. (Wiley, New York, 1981).

[21]J. M. Beebe, B. Kim, J. W. Gadzuk, C. D. Frisbie, and J. G. Kushmerick, Phys. Rev. Lett. **97**, 026801 (2006).

[22]T. Lee, W. Wang, J. F. Klemic, J. J. Zhang, J. Su, and M. A. Reed, J. Phys. Chem. B **108**, 8742 (2004).

[23]D. J. Wold, R. Haag, M. A. Rampi, and C. D. Frisbie, J. Phys. Chem. B **106**, 2813 (2002).

[24]H. Song, H. Lee, and T. Lee, J. Am. Chem. Soc. **129**, 3806 (2007).

[25]V. B. Engelkes, J. M. Beebe, and C. D. Frisbie, J. Phys. Chem. B **109**, 16801 (2005).

[26]Y. Hu, Y. Zhu, H. Gao, and H. Guo, Phys. Rev. Lett. **95**, 156803 (2005).

[27]B. Xu and N. J. Tao, Science **301**, 1221 (2003).